Charge transport and trapping in Cs-doped poly(dialkoxy-*p*-phenylene vinylene) light-emitting diodes

H. H. P. Gommans* and M. Kemerink
Department of Applied Physics, Eindhoven University of Technology, P.O. Box 513, 5600 MB Eindhoven, The Netherlands

G. G. Andersson
Wilhelm-Ostwald-Institut für Physikalische und Theoretische Chemie, Universität Leipzig, Linnéstrasse 2, 04103 Leipzig, Germany

R. M. T. Pijper
Department of Applied Physics, Eindhoven University of Technology, P.O. Box 513, 5600 MB Eindhoven, The Netherlands
(Received 4 November 2003; published 30 April 2004)

Al/Cs/MDMO-PPV/ITO (where MDMO-PPV stands for poly[2-methoxy-5-(3′-7′-dimethyloctyloxy)-1,4-phenylene vinylene] and ITO is indium tin oxide) light-emitting diode (LED) structures, made by physical vapor deposition of Cs on the emissive polymer layer, have been characterized by electroluminescence, current-voltage, and admittance spectroscopy. Deposition of Cs is found to improve the balance between electron and hole currents, enhancing the external electroluminescence efficiency from 0.01 cd A^{-1} for the bare Al cathode to a maximum of 1.3 cd A^{-1} for a Cs coverage of only 1.5×10^{14} atoms/cm^2. By combining *I-V* and admittance spectra with model calculations, in which Cs diffusion profiles are explicitly taken into account, this effect could be attributed to a potential drop at the cathode interface due to a Cs-induced electron donor level 0.61 eV below the lowest unoccupied molecular orbital. In addition, the admittance spectra in the hole-dominated regime are shown to result from space-charge-limited conduction combined with charge relaxation in trap levels. This description allows us to directly determine the carrier mobility, even in the presence of traps. In contrast to recent literature, we demonstrate that there is no need to include dispersive transport in the description of the carrier mobility to explain the excess capacitance that is typically observed in admittance spectra of π-conjugated materials.

DOI: 10.1103/PhysRevB.69.155216 PACS number(s): 73.61.Ph, 68.35.Fx

I. INTRODUCTION

Since the discovery of the luminescent properties of poly(*p*-phenylenevinylene) (PPV) there has been an increasing interest for its application in devices, such as light-emitting diodes (LED's) and solar cells.[1] In order to understand the charge transport properties of this type of π-conjugated material, many investigations have recently been conducted by time of flight (TOF), current-voltage characterization (*I-V*), or admittance spectroscopy.[2–6] These techniques introduce charge carriers either by photoabsorption (photodoping) or injection from metallic contacts. Generally, the interpretation of these experiments suffers from simplifications concerning the metal-polymer interface: abrupt compositional junctions without chemical interaction and alignment of the vacuum energy level are normally assumed.

The electron injecting contact of the LED is typically manufactured by vapor deposition of a low work-function metal onto the polymer layer. By photoelectron spectroscopy chemical (charge-transfer) doping and the subsequent formation of (bi)polaron states[7–11] have been identified upon deposition of alkali(ne) (earth) metals onto π-conjugated systems. Recently, we have demonstrated diffusion up to 200 Å for *submonolayer* deposition of K by ion scattering spectroscopy.[12] Simultaneously, the electroluminescence and efficiency went two orders of magnitude up.

In order to understand how chemical doping and diffusion at the electron injecting contact affect the charge transport and device performance we will study the Cs/MDMO-PPV interface in LED structures by a combination of electrical characterization (electroluminescence, *I-V*, and admittance spectroscopy) with analytical and numerical models and ion scattering spectroscopy.

In the first part of this paper we will discuss the interpretation of the admittance spectra obtained on hole-dominated structures. We demonstrate that an analytical model for the frequency-dependent space-charge-limited behavior in the presence of a single trapping level can describe the observations consistently. This model offers a straightforward and alternative interpretation for the observations to the previously used interpretation in terms of a frequency-dependent mobility in combination with a distribution in transit times.[4,13] At high bias we can also identify minority carrier (electron) injection. Subsequently, we demonstrate how these phenomena are altered by Cs deposition and finally relate the chemical doping to the device performance in terms of charge-carrier dynamics.

II. EXPERIMENTAL

In a glovebox filled with a nitrogen atmosphere poly[2-methoxy-5-(3′,7′-dimethyloctyloxy)-1,4-phenylene vinylene] MDMO-PPV films[14] were prepared by spin coating a 0.7 wt % toluene solution onto an indium tin oxide (ITO) coated glass substrate as described in Ref. 12. The film thickness is typically 170 nm as measured by an alpha stepper. By means of a transfer chamber samples were transported to an

UHV chamber for Cs and Al deposition without being exposed to air. Cs was deposited by evaporation from an alkali-metal dispenser purchased from Saesgetters at about 750 °C. The LED structures (six in each run) were completed by vapor deposition of an 80-nm Al capping layer. The active area for each LED structure amounts 24 mm^2. *I-V* characterization, electroluminescence (EL), and admittance spectroscopy were all conducted *in situ* in the glovebox at a temperature of 20 °C. Admittance spectroscopy in the range of 5 Hz–1 MHz was performed with a Hewlett Packard 4192A impedance analyzer. A small alternating signal v_{ac} of 50 mV was superimposed onto a dc bias v_{dc} up to 10 V. Measurements at different modulation levels ($v_{ac}=10-250$ mV) showed identical results. The results were obtained in five runs at different Cs coverage, which were all repeated once. The, yet extensive, discussion in this paper is restricted to two deposition coverages. The results of the other coverages are entirely consistent with the ones discussed here.

III. RESULTS

A. Al/MDMO-PPV/ITO

In an admittance experiment the charge relaxation driven by a small harmonic voltage modulation v_{ac} is probed. Both the amplitude and the phase difference of the ac current i_{ac} are monitored as a function of frequency f to obtain the complex admittance Y

$$Y(\omega)=i_{ac}/v_{ac}=G(\omega)+i\omega C(\omega),$$

with G conductance, C capacitance, $i=\sqrt{-1}$, and $\omega=2\pi f$ the angular frequency.

Figure 1 gives the capacitance and conductance as a function of frequency at room temperature measured on an Al/MDMO-PPV/ITO structure at different forward bias. At $v_{dc}=0$ V the polymer dielectric response to the alternating field is shown in both the conductance and capacitance spectra and is modeled by the Debye relation

$$\varepsilon(\omega)=\varepsilon_\infty+\frac{\varepsilon_s-\varepsilon_\infty}{1+(i\omega\tau_0)}. \quad (1)$$

This provides us with the real and imaginary components of the permittivity together with a relaxation time τ_0, which describes the relaxation of permanent dipoles present in the polymer (Fig. 2). As the Debye relation clearly is an oversimplification in terms of the local field each dipole feels, the value determined for τ_0 (3.8×10^{-7} s) is overestimated. In addition, at zero bias no charge transport is possible due the built-in potential V_{bi} and hence the conductance is entirely due to the dielectric response.

At $v_{dc}=2$ V, the built-in potential is exceeded and hole injection into the polymer film occurs. As the intrinsic charge-carrier density in the film is negligible compared to the injected charge, the field is entirely determined by the positive space-charge density that has accumulated inside the device. The current limitation by the non-Ohmic behavior of the ITO/MDMO-PPV hole contact may be disregarded in this bias domain, as was demonstrated by Blom *et al.*[15] Modeling of *I-V* curves and impedance spectra of numerous devices confirmed this notion, see also below. Note, however, that the electron contact still is non-Ohmic. The superposition of the harmonically alternating field subsequently results in space-charge waves that redistribute to compensate for these oscillations. When the oscillation period is much longer than the carrier transit time τ_{tr}, i.e., the time the carrier needs to travel from one electrode to the other, the capacitance experiences a negative (or inductive) contribution as a result of this charge relaxation, resulting in a low-frequency capacitance that is 2/3 of its geometrical value. At periods much shorter than τ_{tr} the negative contribution disappears and the original dielectric response is recovered. The same applies for the conductance: as the charges cannot keep

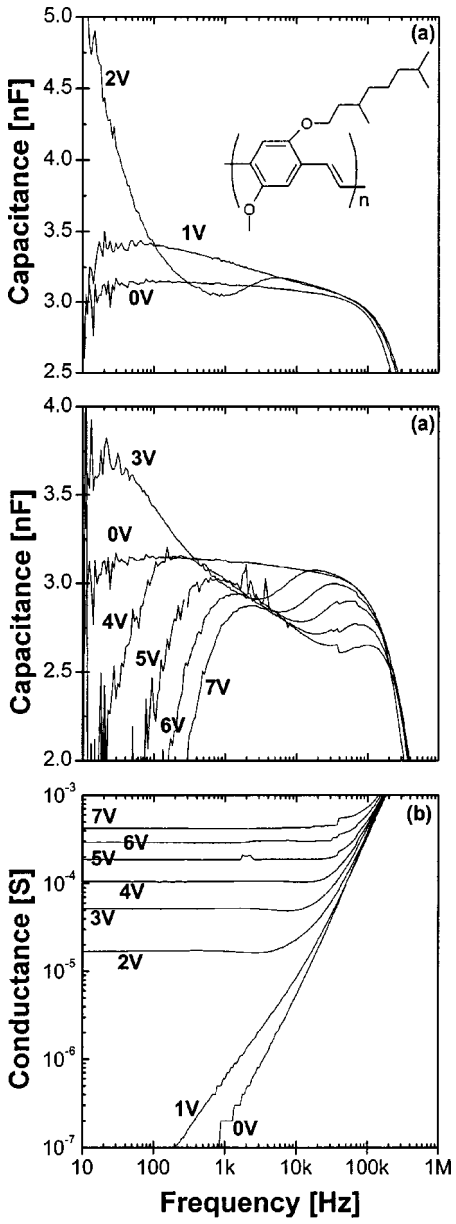

FIG. 1. (a) Capacitance and (b) conductance versus frequency measured at an Al/MDMO-PPV/ITO structure for different forward bias which are indicated in the figure. The inset gives the chemical structure of MDMO-PPV.

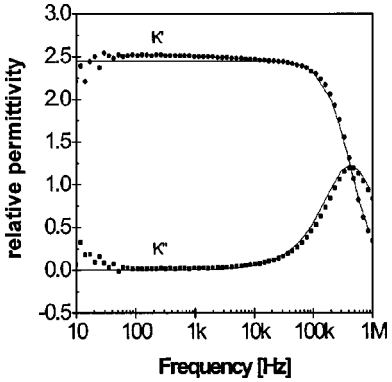

FIG. 2. Plot of the relative complex permittivity $\mathbf{K}=\mathbf{K}'-i\mathbf{K}''$ determined from the admittance $Y=i\omega\varepsilon_0\mathbf{K}$ A/L at zero bias (filled symbols). The dielectric response $\varepsilon(\omega)=\varepsilon_0\mathbf{K}(\omega)$ is approximated by the Debye relation [Eq. (1)] with a dipole relaxation time of 3.8×10^{-7} s (solid line).

up with the alternating field $\omega>1/\tau_{\mathrm{tr}}$ the conductance decreases and the dielectric response takes over. This crossover in admittance spectroscopy is called the transit-time effect and is described by small signal theory for space-charge-limited (SCL) diodes,[16]

$$Y(\omega)=\frac{\varepsilon A}{2L}\frac{\vartheta^3}{\tau_{\mathrm{tr}}}\left[\frac{\vartheta-\sin\vartheta}{(\vartheta-\sin\vartheta)^2+(1-\cos\vartheta-\vartheta^2/2)^2}-i\frac{1-\cos\vartheta-\vartheta^2/2}{(\vartheta-\sin\vartheta)^2+(1-\cos\vartheta-\vartheta^2/2)^2}\right]. \quad (2)$$

A, L, and τ_{tr} are the film surface area, thickness, and hole transit time, respectively.

Here ϑ is the charge-carrier transit angle and equals $\omega\tau_{\mathrm{tr}}$. This classical description is derived from Poisson's law and the continuity equation assuming an Ohmic injecting contact and a field-independent mobility. The transit-time effect is clearly observed in the conductance and capacitance spectra in Fig. 3 and can be used to determine the hole mobility as a function of bias,

$$\tau_{\mathrm{tr}}=\frac{4}{3}\frac{L^2}{(V-V_{\mathrm{bi}})\mu_h}. \quad (3)$$

The oscillations for $\omega\tau_{\mathrm{tr}}\geqslant10$ predicted by Eq. (2) are not observed due to the non-negligible dielectric response at these frequencies that results in a divergence of space charge.[17] At frequencies lower than the reciprocal transit time the observed capacitance significantly deviates from its calculated behavior. This extra contribution to the capacitance has recently been ascribed to dispersive transport due to hopping in a disordered molecular solid.[4,13] Martens *et al.*[4] argued that these hopping events result in both a distribution of transit times as well as a frequency-dependent mobility, $\mu(\vartheta)=1+M(i\vartheta)^{1-\alpha}$ with $0<\alpha<1$. However, as the mobility is directly linked to the transit time via Eq. (3), it seems meaningless to apply separate distribution functions. Moreover, the frequency dependence of the mobility applies only for frequencies higher than the reciprocal transit time, according to Ref. 18, as provided by the authors of Ref. 4.

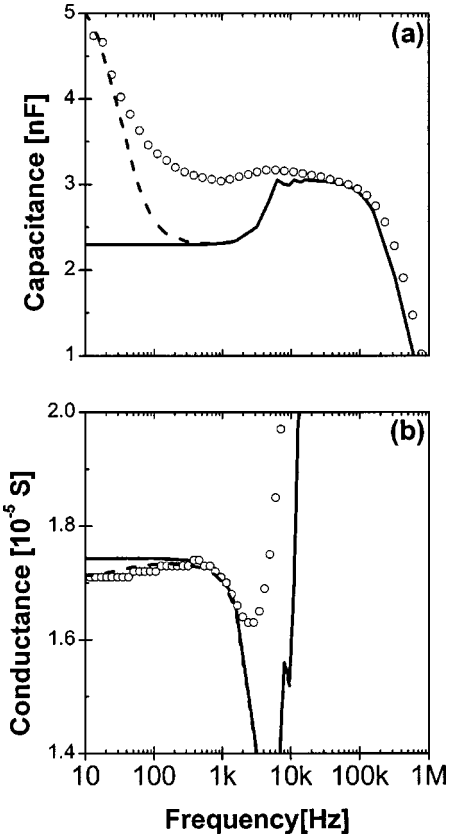

FIG. 3. (a) Capacitance and (b) conductance at $v_{\mathrm{dc}}=2$ V (open symbols). The solid line represents the frequency-dependent SCLC model as calculated in Eq. (2), which gives the hole transit time $\tau_{\mathrm{tr}}=2.15\times10^{-4}$ s. The dashed line includes trap relaxation by a single trap level [Eq. (5)]. The hole lifetime in the valence band and in the trap level are $\tau_v=1.7\times10^{-1}$ s; $\tau_e=5.0\times10^{-3}$ s, respectively.

When characterizing Schottky contacts by admittance spectroscopy, excess capacitances, which exhibit similar frequency behavior as observed in our experiments, are usually interpreted in terms of charge relaxation in trap levels.[19] The excess capacitance is thus explained by traps that become charged. When approaching the trap emission rate by increasing f, charge transfer from the trap starts to lag behind the driving voltage and the out-of-phase component (the excess capacitance) decays, while simultaneously the in-phase component, $G(\omega)$, increases.[19] The theory describing the trapping process in space-charge-limited diodes by a single trapping level was derived by Dascalu[20] and later by Kassing.[21] The equation describing the capture and emission of the charge carrier by a single trap can be linearized and results in both a steady-state and a frequency-dependent trapping parameter θ and $\alpha(\omega)$, respectively, which are given by

$$n_{\mathrm{dc}}+n_{\mathrm{dc},T}=\theta^{-1}n_{\mathrm{dc}},$$
$$n_{\mathrm{ac}}+n_{\mathrm{ac},T}=\alpha(\omega)n_{\mathrm{ac}}, \quad (4)$$
$$\alpha(\omega)=1+\frac{\omega_v}{i\omega+\omega_e}.$$

Here, the subscripts dc, ac, and T refer to the steady state, time-dependent, and trapped values for the charge density. ω_v is the reciprocal of the hole lifetime τ_v in the valence band and ω_e the reciprocal lifetime in the trap τ_e. The expression for the admittance expressed in these parameters becomes[21]

$$Y(\omega)=\frac{\varepsilon A}{2L}\frac{1}{\alpha\tau_{\mathrm{tr}}}\left\{\sum_{k=0}^{\infty}\frac{\Gamma(\theta\alpha+1)}{\Gamma(\theta\alpha+k+2)}\frac{(-i\omega\tau_{\mathrm{tr}})^k}{(k+3)}\right\}^{-1}. \tag{5}$$

Γ is the Euler-gamma function and the frequency dependence of α, according to Eq. (4), is implied. It is easy to show that this expression converges to the original equation for the admittance in the limit $(\theta\rightarrow 1,\alpha\rightarrow 1)$. The gradient in *both* conductance and capacitance can now be fitted with reasonable values for $\tau_e=5.0\times10^{-3}$ s and $\tau_v=1.7\times10^{-1}$ s and agrees qualitatively with the data, see Fig. 3. Note that $1/\tau_e>1/\tau_v$, which is a characteristic of shallow traps. The excess capacitance in Fig. 3 manifests itself in the whole frequency range up to $1/\tau_{\mathrm{tr}}$. This leads to the conclusion that more than one trapping level is present. The description of the capacitance can be made to match the data exactly by inclusion of more than one trapping level. However, the conductance is already accurately modeled by only one trap for which $\tau_e\ll\tau_v$. Note that in the interpretation of Martens *et al.*[4] this low-frequency gradient in the conductance was not included.

The agreement with the data is hardly dependent on the exact value of θ. A variation of θ from 1 to 10^{-5} can be compensated by a change in transit time of only a factor $\sim$2, which is within the experimental error. The admittance spectra of Al/MDMO-PPV/ITO structures thus allow us to simultaneously determine the hole transit time and the trap relaxation as both phenomena are well separated in the frequency domain.

At $v_{\mathrm{dc}}=4$ V a negative contribution to the capacitance sets in, which at higher bias even becomes inductive. This effect has been observed on a range of materials before and is well known to result from minority carrier injection.[22] At high forward bias both charge carriers are injected. At frequencies much lower than the reciprocal dielectric relaxation time but higher than the electron response, the hole density will redistribute to compensate the field modulation. The conductance measured at these frequencies will be entirely due to the hole current density, though possibly suffering from trapping processes. At lower frequencies the electron response sets in and a delayed (= inductive) increase in conductance follows (note the decrease C in Fig. 1).

The frequency at which the capacitance becomes inductive has been explained either in terms of an injection barrier[23] or transit time[24] for the minority carrier. However, as trap relaxation was not taken into account in these references, the actually determined value for the latter parameter becomes arbitrary.

By fitting the conductance spectra to Eq. (5) we obtain the transit time and determine the hole mobility as a function of bias from Eq. (3), see Fig. 4. Here, we neglected the electron contribution to the conductance. The hole mobility clearly

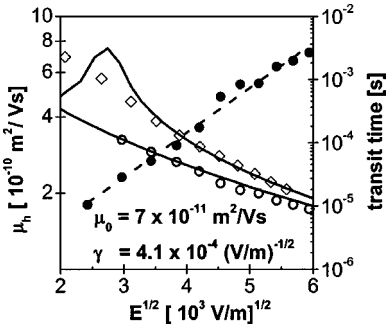

FIG. 4. Mobility (filled circles) determined as a function of bias from the transit-time effect. The Poole-Frenkel behavior $\mu_h=\mu_0\exp(\gamma\sqrt{E})$ is clearly observed. The field-independent mobility $\mu_0=7\times10^{-11}$ m^2/V s and the Poole-Frenkel factor $\gamma=4.1\times10^{-4}$ V/m$^{-1/2}$ are determined from a fit to the data points (dashed line). Open circles represent the transit times as obtained from admittance spectroscopy at an Al/MDMO-PPV/ITO stacking structure and the solid line is the transit time calculated with the steady-state conductivity model. Also included are the transit times obtained from the structure with deposited Cs (4.8×10^{13} atoms/cm^2; open diamonds). The Cs diffusion profile is included in the model as an electron donor level of 0.61 eV below the LUMO level, which was derived from the fit to the measured current density. The agreement is well within the error rate.

exhibits the field dependence typically observed in disordered molecular materials, which follows the Poole-Frenkel law:

$$\mu_h=\mu_0\exp(\gamma\sqrt{E}). \tag{6}$$

Here $\mu_0=7\times10^{-11}$ m^2/V s and $\gamma=4.1\times10^{-4}$ V/m$^{-1/2}$, which is in good agreement with literature.[25] The origin of this Poole-Frenkel behavior is still under debate and various models have been proposed, either assuming energetic disorder due to localized states[26] or structural disorder resulting in stochastic transport.[4,5,13] Note, however, that interpretation of the measured excess capacitance in terms of stochastic transport[4,13] seems ambiguous. The identification of (localized) trap states in the admittance spectra implies that energetic disorder cannot be ignored in the description of the carrier transport. Similar conclusions were obtained from experiments performed on (unsubstituted) PPV. Here, the Poole-Frenkel behavior was ascribed to field-dependent release times from localized states.[3] From thermally stimulated current (TSC) experiments Meier *et al.* identified two levels at 0.03 and 0.18 eV above the valence band, and suggested that the ITO anode could account for this, as these levels were absent in case a Au anode was applied.[27]

The field dependence of the mobility is not explicitly taken into account in the derivation of Eqs. (2) and (5) and one can argue that the field-dependent mobility in Fig. 4 is determined in an inconsistent manner. In order to estimate the error made, the hole transit times are compared to ones obtained from a self-consistent steady-state conductivity model in which the Poole-Frenkel behavior is included. This model will be outlined below. Figure 4 demonstrates that these calculated transit times and the ones determined from

the admittance spectra are in good agreement and hence the inconsistency in the determination for the mobility is of negligible importance.

The steady-state model is based on the model presented in Refs. 28 and 29. It treats charge injection and bulk transport on an equal level, which implies that no *a priori* assumptions about the dominance of either process need to be made. The bulk transport is described by the well-known drift equation $j=n_{\mathrm{dc}}q\ \mu(E)\ E$, where all parameters but q may depend on the position z between the electrodes and $\mu(E)$ is given by Eq. (6). Carrier injection is described in terms of hopping injection into a Gaussian distribution of transport sites.[30] The field distribution $E(z)$ is obtained by simultaneously solving the Poisson equation. Apart from the charge density due to the mobile electrons and/or holes, charge density may also result from the presence of doping or trapping states. The local degree of dopant ionization follows immediately from the position of the (local) hole or electron quasi-Fermi-level. The latter is obtained from the relation

$$n_{\mathrm{dc}}(z)=\int_{-\infty}^{\infty} dE\, g(E) f(E-E_F). \tag{7}$$

with $g(E)=g_0(2\pi\sigma^2)^{-1/2}\exp(-E^2/2\sigma^2)$, the Gaussian density of states with width σ, and $f(E-E_F)$ the Fermi distribution function that is approximated by a step function. In Eq. (7), the center of the lowest unoccupied molecular orbit (LUMO) level is taken as zero energy. A similar expression holds for holes, with E replaced by $E-E_g$ in which E_g is the (single-particle) band gap of the organic semiconductor. The occupation θ of a shallow trap level under a Gaussian transport level is given by

$$\theta=\frac{N}{N_T}\exp\left[\frac{1}{2}\left(\frac{\sigma}{kT}\right)^2-\frac{|E_{\mathrm{tr}}-E_T|}{kT}\right], \tag{8}$$

where σ equals 0.12 eV for MDMO-PPV.[31] N and N_T are the number of transport and trap sites, respectively, and $E_{\mathrm{tr}}-E_T$ is the energy of the trap level.

We use μ_0 and γ derived from the admittance experiments measured at the Al/MDMO-PPV/ITO structure, and the only unknown parameter, the built-in potential, is determined to be 1.2 V by optimizing the correspondence to the measured current density (Fig. 5). The model reduces to space-charge-limited behavior when the injection barrier is set below 0.3 eV.[32] Notice that the steady-state conductivity can be accurately described without including a trapping level. This indicates that the trap density is either very low or indeed shallow, as was determined by the admittance spectra. The reproducibility in hole mobility (about a factor 2 in this bias range) is mainly determined by the variation in polymer layer thickness.

B. Al/Cs/MDMO-PPV/ITO

The effect of Cs deposition on the electroluminescence is demonstrated in Fig. 6. The luminescence is continuously enhanced with Cs coverage starting from 5 $\mathrm{cd\,m^{-2}}$ up to 2500 $\mathrm{cd\,m^{-2}}$ at 10-V bias and its onset is reduced from 5 V to about 2 V. The current density as a function of bias initially decreases with Cs deposition. At higher coverage the current density increases again (Fig. 5). The current onset shifts from 1.0 to 1.4 V. The efficiency (Fig. 6) starting at a maximum value of 0.01 $\mathrm{cd\,A^{-1}}$ converges to a value of 1.3 $\mathrm{cd\,A^{-1}}$ and cannot not be altered upon further deposition. The energy-resolved electroluminescence spectra of these structures show a shift of the spectral maximum towards

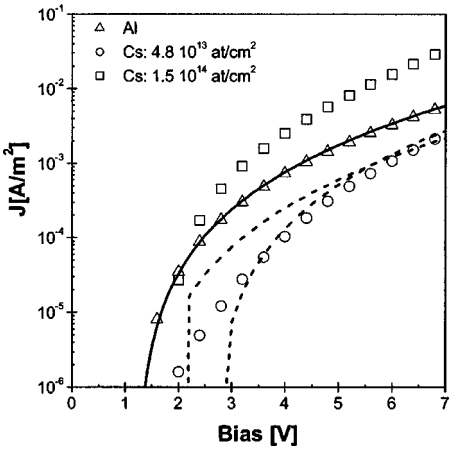

FIG. 5. Current density-voltage characteristics at various Cs deposition coverages: 4.8×10^{13} (circle) and 1.5×10^{14} (square) atoms/cm^2 and without Cs (triangle). For the latter structure the conductivity (solid line) is accurately described by the steady-state model. At a Cs coverage of 4.8×10^{13} atoms/cm^2 we calculated the effect of a hole trapping level (upper dashed line) or an electron donor level (lower dashed line).

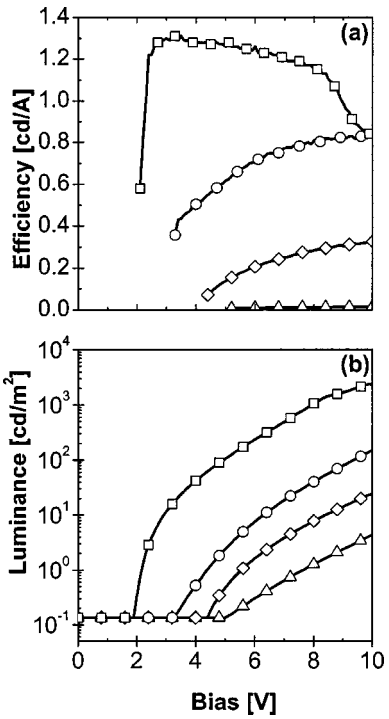

FIG. 6. (a) Efficiency and (b) electroluminescence (EL) versus bias on Al/Cs/MDMO-PPV/ITO structures with varying Cs deposition coverage: 4.2×10^{13} (diamond), 4.8×10^{13} (circle), and 1.5×10^{14} (square) atoms/cm^2 and without Cs (triangle).

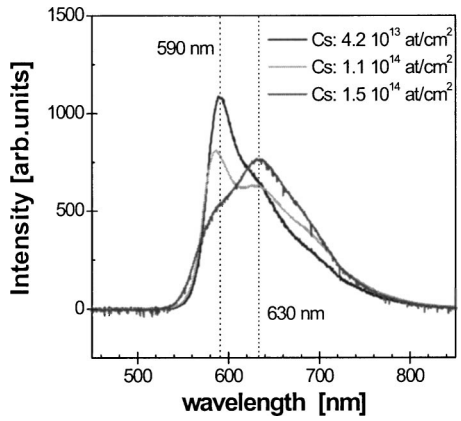

FIG. 7. Electroluminescence spectrum as a function of Cs deposition.

lower energies (redshift) as a function of deposition (Fig. 7). This suggests that recombination occurs close at the interface where Cs is deposited and the electronic structure is altered, which is anticipated when modifying the conduction from hole dominated to double injection.

Ion scattering spectroscopy clearly demonstrates the diffusion of Cs atoms up to 150 Å into the polymer layer as illustrated in Fig. 8. For the experimental details and a description of the used technique we refer to Ref. 12 in which similar results were obtained for the deposition of K onto MDMO-PPV. Cs was not detected at the polymer surface, indicating complete diffusion into the polymer. Integration of these spectra yields the total deposited amount as given in the caption to Fig. 8.

The admittance measurements performed on the structure with a Cs coverage of 4.8×10^{13} atoms/cm^2 demonstrate a decreased hole conductance, in correspondence with the I-V characterization (Fig. 9). Both the excess capacitance and the gradient in conductance become more pronounced compared

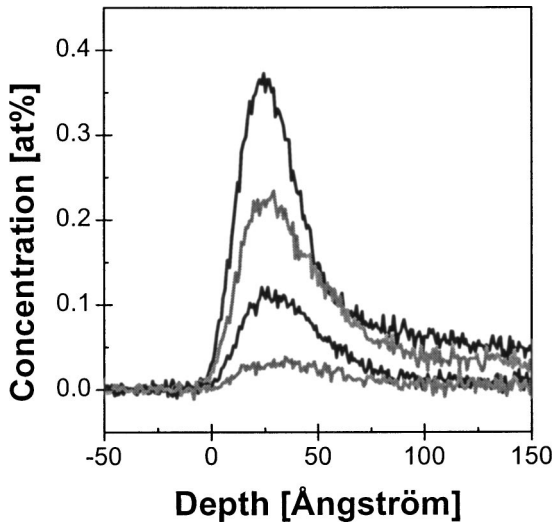

FIG. 8. Cs diffusion profiles obtained by NICISS. The total deposition is calculated by integration of the spectra and amounts (from top to bottom) to 1.5×10^{14}, 1.1×10^{14}, 4.8×10^{13}, and 1.7×10^{13} atoms/cm^2.

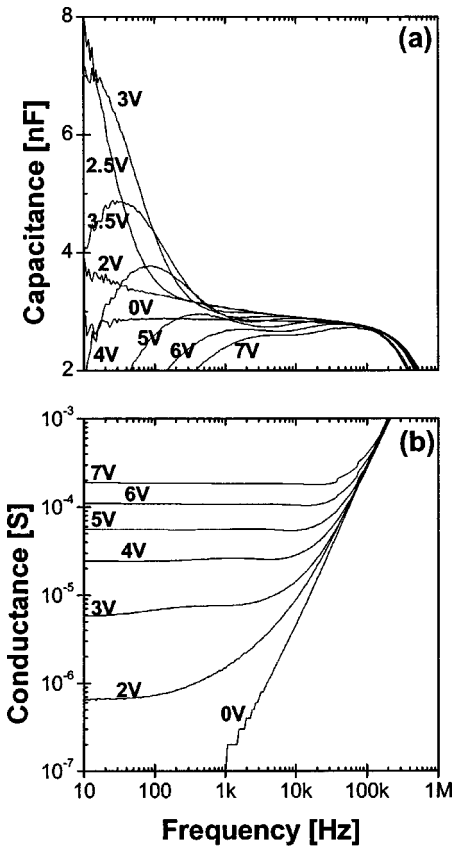

FIG. 9. (a) Capacitance and (b) conductance versus frequency on an Al/Cs/MDMO-PPV/ITO structure for different forward bias, which are indicated in the figure. Cs deposition coverage is 4.8×10^{13} atoms/cm^2.

to the spectra without Cs. This is mostly reflected in the hole lifetime in the valence band which is an order of magnitude smaller than for the Al/MDMO-PPV/ITO structure. The crossover due to the transit-time effect is obscured in the admittance spectra at low bias due to this trap relaxation (Fig. 10). At higher bias the transit-time effect reappears and the conduction spectra demonstrates an increase in the hole transit time compared to the Al/MDMO-PPV/ITO structures. The corresponding lifetimes in the valence and trap level for this Al/Cs/MDMO-PPV/ITO structure at 3-V bias are $\tau_v = 9.0\times10^{-3}$ s and $\tau_e = 1.9\times10^{-3}$ s (Fig. 10) and the hole transit time as a function of bias is plotted in Fig. 4.

At 6 V the minority carrier features in the admittance spectra are clearly visible and resemble the behavior without Cs, though the absolute value for the (hole-dominated) conductance in this frequency domain is much lower, see Fig. 11.

At 1.5×10^{14} atoms/cm^2 coverage and zero bias we observe an increased conductance and a capacitive contribution up to 2×10^4 Hz, see Figs. 12 and 13. In the whole bias range, i.e., up to 7 V, the transit time crossover for holes can no longer be identified in the conduction spectra. Hence, we conclude that this space-charge effect is completely perturbed by the presence of either hole trapping levels or electron transport. We observe that the inductive contribution

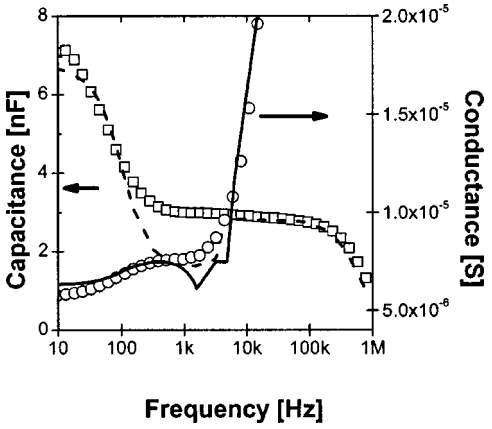

FIG. 10. Conductance and capacitance versus frequency on an Al/Cs/MDMO-PPV/ITO structure with deposition coverage 4.8×10^{13} atoms/cm^2 at 3-V bias (open symbols). Also shown are the real and imaginary parts of Eq. (5) $\tau_{tr}=2.24\times10^{-4}$ s, $\theta=10^{-5}$, $\tau_v=9.0\times10^{-3}$ s, and $\tau_e=1.9\times10^{-3}$ s.

to the capacitance shifts towards higher frequencies ($\sim10^4$ Hz at 6 V), which indicates an enhanced electron transport.

IV. DISCUSSION

Photoelectron spectroscopy (PES) and electron energy-loss spectroscopy (EELS) studies have demonstrated the charge transfer and the subsequent formation of gap states upon deposition of alkali- and alkaline-earth metals onto π-conjugated systems.[7–11] These states have been identified as polaron and bipolaron states (see the inset of Fig. 14). The lower state above the highest occupied molecular orbital (HOMO) is double occupied while the upper state below the lowest unoccupied molecular orbital (LUMO) is single (double) occupied in case of a (bi)polaron. Below, these PES results are employed to interpret our admittance experiments. The Cs concentrations are below one monolayer coverage and consequently it seems reasonable to assume that complete charge transfer has occurred.

The decreased current density at 4.8×10^{13} atoms/cm^2 coverage, and consequently also the increased hole transit

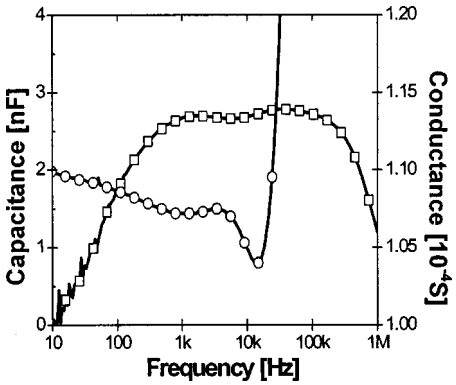

FIG. 11. Conductance (circles) and capacitance (squares) versus frequency on an Al/Cs/MDMO-PPV/ITO structure with deposition coverage 4.8×10^{13} atoms/cm^2 at 6-V bias.

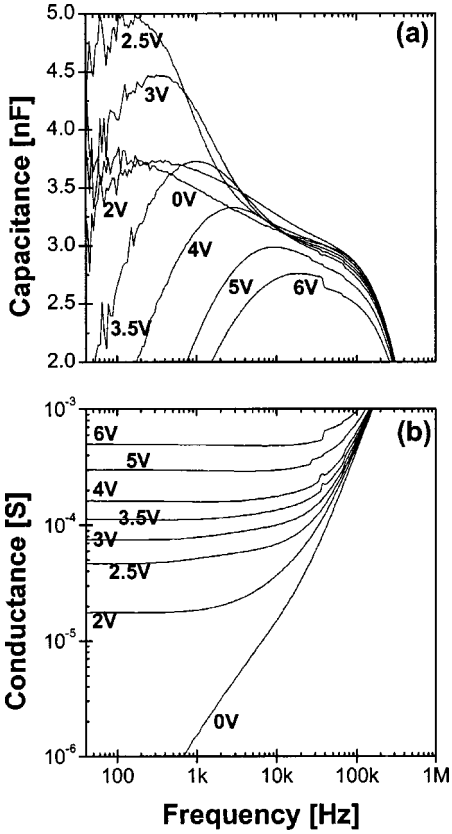

FIG. 12. (a) Capacitance and (b) conductance versus frequency on an Al/Cs/MDMO-PPV/ITO structure for different forward bias. Cs deposition coverage is 1.5×10^{14} atoms/cm^2.

time, may either originate from Coulomb scattering, trapping, or doping at the polymer cathode interface. Of these possibilities Coulomb scattering may be neglected as, even in the vicinity of the Al layer, the mean free path of approximately 3 nm is much smaller than the inter-alkali-atom distance. Charging of either electron donors or hole trapping states will lead to additional band bending and hence cause a significant fraction of the potential difference to drop in the interface layer. In this case a change in transit time does therefore not necessarily imply a change in mobility, but rather a change in field distribution in the device. In order to quantify this proposition we extended the model to calculate the steady-state conductivity by taking into account the measured Cs profile as a distribution of either electron donors or hole traps. By only adjusting the energy of the trapping/doping level, good agreement with the measured steady-state conductivity is obtained. These doping and/or trapping levels are approximated to be independent of concentration, as we assume no interaction among the Cs sites at such low coverage. The results are depicted as dashed lines in Fig. 5. We observe a reduced (hole dominated) current density in both cases. The inclusion of a trapping level, however, exhibits a reduced current density only at high bias, which can be understood from the fact that charging of the traps may only occur *after* hole injection sets in. In contrast, doping states are immediately charged upon deposition: donated electrons will minimize their energy by diffusing to the Al electrode,

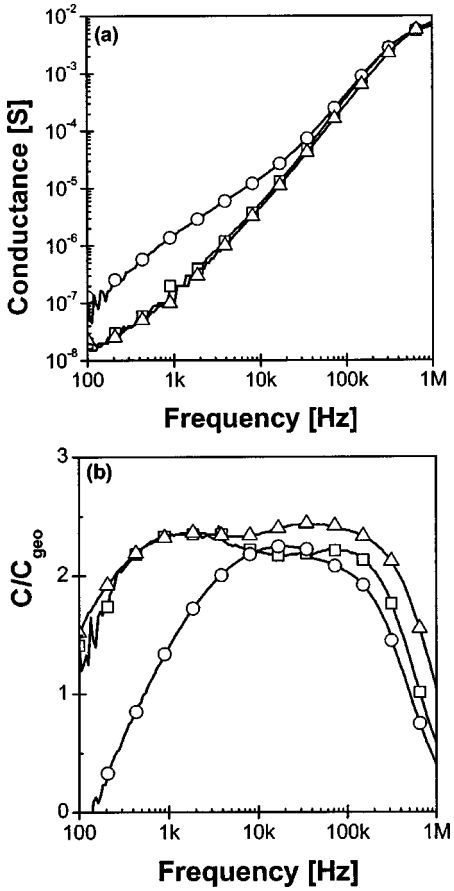

FIG. 13. (a) Conductance at zero bias for an Al/MDMO-PPV/ITO structure (squares) and for the Al/Cs/MDMO-PPV/ITO structures with 4.8×10^{13} (triangles) and 1.5×10^{14} at/cm^2 (circles) Cs deposition coverage. (b) Normalized capacitance C/C_{geo} measured at 6-V bias for these structures, where C_{geo} represents the geometrical capacitance.

creating a positively charged background. Consequently, the current density will be reduced over the whole bias range. Apart from the region directly at the current onset, a donor level at 0.61 eV below the LUMO level gives the best agreement with the measured current density. Hence we tentatively attribute the field modification at the MDMO-PPV/Al interface to a Cs-induced electron donor level (Fig. 14), which then accounts for the observed increase in hole transit time. The increased hole transit times observed in the admittance spectra, shown in Fig. 4, compare favorably with the ones calculated using this steady-state model.

The increased conductance and capacitance at zero bias observed at 1.5×10^{14} atoms/cm^{-2} coverage (Fig. 13) confirm the identification of Cs-induced donor states. Upon deposition the Fermi level in the originally intrinsic layer moves from the gap into these states. Electrons then redistribute by tunneling or diffusion in the (possibly Cs induced) gap states to compensate for the oscillating field. This redistribution explains the higher capacitance as the total dipole moment increases due to the mobile electrons. When the frequency is increased, the average distance electrons can travel is reduced and hence the contribution from this enhanced dipole moment disappears. When $\omega\sim1/\tau_e$ the

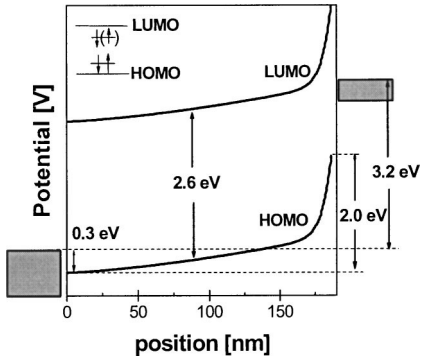

FIG. 14. Calculated potential distribution through the polymer layer (186 nm) at 3.2-V bias with a donor concentration corresponding to the diffusion profile obtained for the 4.8×10^{13} atoms/cm^2 Cs deposition and an energy level of 0.61 eV below the LUMO. The left side corresponds with the ITO contact. The inset schematically pictures the (bi)polaron level in the band gap.

trapped charge carriers cannot follow the harmonic oscillations and the out-of-phase component partly changes into an in-phase contribution.[19] This we observe in the conductance spectrum for the whole frequency range up to 2×10^4 Hz. Cs inducing only a neutral hole trapping level (at 0 V) cannot account for these features in the admittance spectra, as the hole capture and emission rate cannot be probed below the onset of hole injection. The inductive contribution to the capacitance at 6 V is maintained up to higher frequencies as compared to samples with lower Cs coverage, which is indicative for an enhanced electron transport. This confirms the enhanced field at the interface, which indeed should result in an increased electron injection and/or higher electron mobility (Fig. 14). This interpretation is in good correspondence with the observed increase in the steady-state conductivity for these LED structures.

The excess capacitance at low bias that we describe by the charge relaxation in a trap level is clearly affected by Cs doping. We observe an increased excess capacitance, which is reflected in a reduced value for the hole lifetime in the valence band. The observed ratio $\omega_v/\omega_e<1$ for moderate Cs doping indicates that shallow traps dominate the conduction spectra. This is not contradicting the steady-state calculations, from which we claimed to observe the effect of a Cs-induced donor level. The conductivity at 4.8×10^{13} atoms/cm^2 remains hole dominated and hence *dispersion* in the admittance spectra at 2–3-V bias can only be expected from hole relaxation in trap levels. However, the *decline* in the steady-state current density due to field modification in the polymer layer is attributed to an electron donating level. The enhanced trapping features in the admittance spectra as a result of Cs deposition can be understood from either an increasing number of trap states or from the increased field at the Cs-doped interface, which remains a subject for further investigations.

Admittance spectroscopy thus successively demonstrates an increased hole transit time and an enhanced electron transport with Cs deposition, which is confirmed by steady-state conductivity measurements and modeling. The improved charge balance is reflected in the enhanced electrolu-

minescence for Al/Cs/MDMO-PPV/ITO structures. Moreover, exciton dissociation by the metal-induced gap states as observed by Park *et al.*[33] apparently is of secondary importance and we conclude that Cs *diffusion* is in fact favorable for current balancing and hence electroluminescence.

We analytically describe the excess capacitance and the conductance *simultaneously* by taking into account the (majority carrier) transit time effect combined with a single trap level. This interpretation differs from recently published literature.[4,13] In our opinion, the explanation of the excess capacitance by introducing an extra set of parameters that take into account the spread in hole transit times as well as a frequency-dependent mobility, seems unnecessary and can in fact be ruled out by the arguments given in former sections. We also demonstrate that deriving directly the electron mobility from the spectra[24] seems ambiguous.

The phenomenological dependence of excess capacitance on minority carrier injection was first demonstrated by Werner *et al.*[34] We confirm that the capacitance is highly dependent on fabrication of the minority carrier injection contact. However, we describe the excess capacitance by the lifetimes of the hole transport and trap level. Minority carrier injection in principle leads to recombination, which was not observed below 4-V bias for devices without Cs deposition. In fact, excess capacitances were also demonstrated in single carrier devices for either hole transport[4] as well as electron transport.[13] It remains to be determined how these lifetimes are affected by minority carrier injection.

V. CONCLUSION

Quantitative agreement is found between admittance experiments and the analytical description of the frequency-dependent space-charge-limited transport taking into account trap relaxation in Al/MDMO-PPV/ITO devices. We also show that the field-independent mobility approximation in this model is applicable within the experimental limitations and this technique can thus be applied to directly determine carrier mobilities in the space-charge-limited conduction (SCLC) regime, even in the presence of trap levels.

From the electronic transport characterization we can directly distinguish between two processes that result in an enhanced electroluminescence with Cs deposition in the submonolayer regime. We identify an increase in the hole transit time at a doping concentration of 4.8×10^{13} atoms/cm^2 and additionally an improved electron injection. The latter was concluded from a shift of the inductive contribution towards higher frequency at concentrations $\geqslant 1.5\times10^{14}$ atoms/cm^2. We attribute both phenomena to a potential drop near the cathode interface as a result of chemical doping by the alkali-metal species. A steady-state model including doping was developed to calculate the current density as an explicit function of the two charge densities and mobilities at each position in the polymer layer. Good agreement with both the hole transit times derived from admittance spectroscopy and the *I-V* characterization was obtained.

This proves that the condition for the alignment of energy levels between the LUMO and metal work function for electron injection may be relaxed by doping of the polymer surface layer, for which submonolayer concentrations already suffice. In principle, even noble metals, which are less sensitive to oxygen and water in the atmosphere, can act as an electron injection contact.

ACKNOWLEDGMENTS

We thank A. W. Denier van der Gon who initiated this work but did not live to see the results presented in this paper. We also thank H. B. Brom for making available the HP 4195A impedance analyzer. This research was supported by grants from the Dutch Foundation for Material Research (FOM).

*Author to whom correspondence should be addressed. Electronic mail: h.h.p.gommans@tue.nl

[1] J. H. Burroughes, D. D. C. Bradley, A. R. Brown, R. N. Marks, K. Mackay, R. H. Friend, P. L. Burn, and A. B. Holmes, Nature (London) **347**, 539 (1990).
[2] S. H. Kim, T. Zyung, H. Y. Chu, L.-M. Do, and D.-H. Hwang, Phys. Rev. B **61**, 15854 (2000).
[3] G. Juška, K. Arlauskas, M. Viliūnas, K. Genevičius, R. Österbacka, and H. Stubb, Phys. Rev. B **62**, R16235 (2000).
[4] H. C. F. Martens, H. B. Brom, and P. W. M. Blom, Phys. Rev. B **60**, R8489 (1999).
[5] P. W. M. Blom and M. C. J. M. Vissenberg, Phys. Rev. Lett. **80**, 3819 (1998).
[6] H. Meyer, D. Haarer, H. Naarmann, and H. H. Hörhold, Phys. Rev. B **52**, 2587 (1995).
[7] E. Ettegui, H. Razafitrimo, Y. Gao, B. R. Hsieh, W. A. Field, and M. W. Ruckman, Phys. Rev. Lett. **76**, 299 (1996).
[8] D. Steinmüller, M. G. Ramsey, and F. P. Netzer, Phys. Rev. B **47**, 13323 (1993).
[9] M. Fahlman, D. Beljonne, M. Lögdlund, R. H. Friend, A. B. Holmes, J. L. Brédas, and W. R. Salaneck, Chem. Phys. Lett. **214**, 327 (1993).
[10] G. Iucci, K. Xing, M. Lögdlund, M. Fahlman, and W. R. Salaneck, Chem. Phys. Lett. **244**, 139 (1995).
[11] J. Birgerson, M. Fahlman, P. Bröms, and W. R. Salaneck, Synth. Met. **80**, 125 (1996).
[12] H. H. P. Gommans, A. W. Denier van der Gon, G. G. Andersson, L. J. van IJzendoorn, R. M. T. Pijper, and H. H. Brongersma, J. Appl. Phys. **94**(9), 5756 (2003).
[13] S. Berleb and W. Brütting, Phys. Rev. Lett. **89**, 286601-1 (2002).
[14] D. Braun, E. G. J. Staring, R. C. J. E. Demandt, G. L. J. Rikken, Y. A. R. R. Kessener, and A. H. J. Venhuizen, Synth. Met. **66**, 75 (1994).
[15] P. W. M. Blom, M. J. M. de Jong, and J. J. M. Vleggaar, Appl. Phys. Lett. **68**(23), 3308 (1996).
[16] J. Shao and G. T. Wright, Solid-State Electron. **3**, 291 (1969).
[17] R. Heidemann, D. Jäger, and R. Kassing, Phys. Status Solidi A **44**, 191 (1977).
[18] H. Böttger and V. V. Bryksin, *Hopping Conduction in Solids* (Akademie-Verlag, Berlin, 1985).
[19] P. Blood and J. W. Orton, *The Electrical Characterization of Semiconductors: Majority Carriers and Electron States* (Academic Press, San Diego, 1992).

[20] D. Dascalu, Int. J. Electron. **21**, 183 (1966).
[21] R. Kassing, Phys. Status Solidi A **28**, 170 (1975).
[22] M. Ershov, H. C. Liu, L. Li, M. Buchanan, Z. R. Wasilewski, and A. K. Jonscher, IEEE Trans. Electron Devices **45**, 2196 (1998). This article gives an extensive reference overview.
[23] F. Lemmi and N. M. Johnson, Appl. Phys. Lett. **74**, 251 (1999).
[24] H. C. F. Martens, J. N. Huiberts, and P. W. M. Blom, Appl. Phys. Lett. **77**, 1852 (2000).
[25] P. W. M. Blom and M. J. M. de Jong, IEEE J. Sel. Top. Quantum Electron. **4**, 105 (1998).
[26] H. Bässler, Phys. Status Solidi B **175**, 15 (1993); D. H. Dunlap, P. E. Paris, and V. M. Krenke, Phys. Rev. Lett. **77**, 542 (1996); S. V. Novikov, D. H. Dunlap, V. M. Krenke, P. E. Paris, and A. V. Vannikov, *ibid.* **81**, 4472 (1998).
[27] M. Meier, S. Karg, K. Zuleeg, W. Brütting, and M. Schwoerer, J. Appl. Phys. **84**, 87 (1998).
[28] M. Kemerink, P. Offermans, P. M. Koenraad, J. K. J. van Duren, R. A. J. Janssen, H. W. M. Salemink, and J. H. Wolter, Phys. Rev. Lett. **88**, 2404 (2002).
[29] M. Kemerink, S. F. Alvarado, P. Müller, P. M. Koenraad, H. W. M. Salemink, J. H. Wolter, and R. A. J. Janssen (unpublished).
[30] V. I. Arkhipov, E. V. Emelianova, Y. H. Tak, and H. Bässler, J. Appl. Phys. **84**, 848 (1998); V. I. Arkhipov, U. Wolf, and H. Bässler, Phys. Rev. B **59**, 7514 (1999).
[31] T. van Woudenbergh and P. W. M. Blom, Appl. Phys. Lett. **82**, 985 (2003).
[32] The steady-state equation for SCLC, also called the Mott-Gurney square law: $J=\frac{9}{8}(\varepsilon/L^3)\mu_h(V-V_{bi})^2$ in combination with Eq. (6) is in good agreement with the I-V data on the Al/MDMO-PPV/ITO structure (not shown). This indicates that our model indeed converges to this classical description.
[33] Y. Park, V.-E. Choong, B. R. Hsieh, C. W. Tang, and Y. Gao, Phys. Rev. Lett. **78**, 3955 (1997).
[34] J. Werner, A. F. J. Levi, R. T. Tung, M. Anzlowar, and M. Pinto, Phys. Rev. Lett. **60**, 53 (1988).